Effects of titanium concentration on microstructure and mechanical properties of high-purity vanadium alloys

Materials & Design 224 (2022) 111390

Contents lists available at ScienceDirect

Materials & Design

journal homepage: www.elsevier.com/locate/matdes

Effects of titanium concentration on microstructure and mechanical properties of high-purity vanadium alloys

Jingjie Shen [a,*], Takuya Nagasaka [a], Masayuki Tokitani [a], Takeo Muroga [a], Ryuta Kasada [b], Seiji Sakurai [c]

[a] National Institute for Fusion Science, 322-6 Oroshi-cho, Toki, Gifu 509-5292, Japan
[b] Institute for Materials Research, Tohoku University, 2-1-1 Katahira, Aoba-ku, Sendai, Miyagi 980-8577, Japan
[c] Taiyo Koko Co., Ltd., 1-1-39 Isobe-dori, Chuo-ku, Kobe, Hyogo 651-0084, Japan

HIGHLIGHTS

- High-purity vanadium alloys were developed for structural materials in fusion reactor.
- Precipitates form when Ti concentration is about 1 wt% in high-purity V-4Cr-xTi alloys.
- Solid solution strengthening is prominent and increases as Ti concentration rises.
- 1 wt% Ti addition is presumably proper from the viewpoint of scavenging effect and precipitation strengthening.

GRAPHICAL ABSTRACT

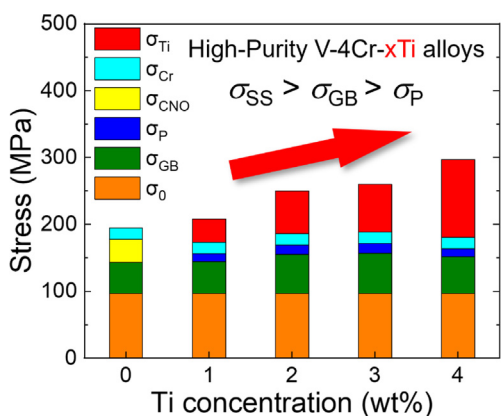

ARTICLE INFO

Article history:
Received 27 April 2022
Revised 31 October 2022
Accepted 17 November 2022
Available online 18 November 2022

Keywords:
High-purity vanadium alloy
Ti concentration
Precipitation
Tensile properties
Strengthening mechanisms

ABSTRACT

Effects of Ti concentration on microstructure and mechanical properties of high-purity V-4Cr-xTi alloys have been studied by means of scanning electron microscopy, transmission electron microscopy, Vickers hardness and tensile tests. Results show that precipitation occurs with 1 wt% Ti addition and above, whose diameter gradually increases as Ti concentration rises. Vickers hardness and tensile strength increase with increasing Ti concentration. Moreover, strengthening mechanisms consisting of solid solution strengthening (σ_{SS}), grain boundary strengthening (σ_{GB}), and precipitation strengthening (σ_P) are theoretically estimated. The strength contribution sequence is $\sigma_{SS} > \sigma_{GB} > \sigma_P$. Solid solution strengthening from Ti increases with increasing Ti concentration, and precipitation strengthening is not significantly dependent on Ti concentration. Additionally, 1 wt% Ti is probably sufficient to scavenge the interstitial impurities and provide comparable precipitation strengthening with V-4Cr-4Ti alloy.

1. Introduction

Low-activation vanadium alloys have been considered as candidate structural materials for the first wall/blanket applications in fusion reactors [1–4]. V-4Cr-4Ti alloy has been selected as the most promising alloy composition with a level of interstitial impurities (C, N and O) of ~1000 wppm in 1990s [5,6]. Although interstitial impurities are beneficial to enhance the strength of vanadium alloys by solid solution strengthening and/or precipitation strengthening, they give rise to loss of ductility at high concentrations [7–10]. Moreover, irradiation-induced defects, clusters and/

* Corresponding author.
E-mail address: shen.jingjie@nifs.ac.jp (J. Shen).

https://doi.org/10.1016/j.matdes.2022.111390
0264-1275/

or precipitates result in hardening and embrittlement of vanadium alloys containing interstitial impurities after ion/neutron irradiation [11–16]. It is expected that reduction of these interstitial impurities should have a good effect on the irradiation damage resistance of vanadium alloys. Thanks to the improvement of manufacturing technology, high purity vanadium alloys [17–21] containing much lower interstitial impurities, ~300 wppm, have been developed at National Institute for Fusion Science (NIFS) in collaboration with Japanese industries. Furthermore, Ti, an alloying element in vanadium alloys, is added, firstly, to scavenge the interstitial impurities by forming Ti(CON) precipitates and keep impurity level in the matrix low; secondly, to enhance the mechanical properties via solid solution strengthening; and thirdly, to improve the fabricability and irradiation swelling resistance [22]. Loomis et al. [23] demonstrated that the swelling of V-Ti alloys and V-Cr-Ti alloys under neutron irradiation at 420 and 600 ℃ was significantly dependent on Ti concentration, and V-Cr-Ti alloys with higher than 3 wt% Ti showed better swelling resistance. Similarly, Matsui et al. [24] and Fukumoto et al. [25] reported that Ti addition showed remarkable swelling resistance in V-Fe alloys and 3 at% Ti addition evidently suppressed the cavity formation under irradiation at 380 – 615 ℃. On the other hand, Ti produces a long-lived radioactive isotopes under fusion irradiation environments, ^{42}Ar [26], whose half-life decay period is ~32 years. It is therefore disadvantageous to recycling and waste management after shutdown of the fusion reactors. Cheng [27] reported that the allowable Ti concentration in vanadium alloys should be lower than 1.4 wt% to reduce the cooling time to less than 100 years as a hands-on recycling level. Aiming at shortening the recycling period of V-Cr-Ti alloys after shutdown of the fusion reactors, it is necessary to keep the level of high-activation elements, interstitial impurities, and Ti concentration as low as possible. High-purity vanadium alloys with much lower concentration of high-activation elements and interstitial impurities were fabricated. To further reduce the cooling time of V-Cr-Ti alloys, minimizing Ti concentration is considered. However, there was no systematic research on the influence of low-Ti levels (~4 wt%) in high-purity vanadium alloys. In the present study, the effects of Ti concentration on microstructure and mechanical properties have been investigated.

2. Experimental

2.1. Materials

High-purity vanadium alloys with nominal composition of V-4Cr-xTi (x = 0, 1, 2, 3, and 4 in wt%) were made by arc-melting process, which are hereafter marked as V-4Cr, V-4Cr-1Ti, V-4Cr-2Ti, V-4Cr-3Ti, and V-4Cr-4Ti alloys. The chemical composition of specimens is listed in Table 1.

Each ingot was sealed in a vacuum stainless steel container, and then hot forged in the temperature range of about 1000 – 1200 ℃. Afterward, the specimens were machined to remove the deformed stainless-steel container and finally rolled at room temperature from about 4 mm to 0.25 mm in thickness. Dog-bone shape tensile specimens with a gauge size of 5 × 1.2 mm and discs with a diameter of 3 mm were punched out from the cold rolled sheets. Specimens were mechanically ground with SiC sandpapers from grit No. 400 to No. 800. Subsequently, the specimens were put into a tantalum box wrapped with zirconium foil and annealed in a vacuum at 1000 ℃ for 1 h.

2.2. Microstructure characterization

As for the grain size estimation, the annealed specimens were electro-polished at 13 V in a solution of 20 vol% H_2SO_4 and 80 vol% CH_3OH at ~5 ℃, and then etched in 25 vol% HF, 25 vol% HNO_3 and 50 vol% H_2O at room temperature. The etched grains were characterized by JEOL JSM-5600 scanning electron microscope (SEM) at an accelerating voltage of 20 kV. Five SEM images were taken on the rolling plane under 400× magnification for each specimen to estimate the grain size. The average grain size was determined via the linear intercept method, and the standard deviation was set as an error. Besides, the precipitates in the matrix were observed by JEOL JEM-2800 transmission electron microscope (TEM) at 200 kV. TEM specimens were prepared by twin-jet electro-polishing in Struers TenuPol-5. Several TEM images were taken to get plenty of precipitates for quantitative estimation by GATAN DigitalMicrograph. The average diameter was obtained by measuring each area of several hundred precipitates via ImageJ under an assumption that all precipitates are spherical, and the standard deviation was set as an error. Regarding the number density of precipitates, thickness of the observed areas was approximately estimated at two-beam conditions by counting the thickness fringes.

2.3. Vickers hardness and tensile tests

Vickers hardness tests were conducted at room temperature by Mitutokyo HM-200 with a load of 0.3 kg for a dwell time of 30 s. The average hardness value was obtained by measuring 10 points, and the standard deviation was set as an error. Three tensile specimens were prepared for each alloy. The thickness of the gauge was averaged by measuring three times with a micrometer caliper, and the width was measured by a laser microscope. Tensile tests were carried out at room temperature with a strain rate of 6.67×10^{-4} s^{-1}, and the displacement during test was recorded by linear variable displacement transformers. After tensile tests, tensile properties, such as yield stress, ultimate tensile stress, uniform elongation, and total elongation, were obtained from engineering stress–strain curves.

3. Results

3.1. Microstructure

3.1.1. Grain size

Fig. 1 shows the SEM images of vanadium alloy with various Ti concentration. Equiaxial grains can be clearly seen in all the spec-

Table 1
The chemical composition of high-purity vanadium alloys (wt%).

Specimens	Cr	Ti	C	N	O	V
V-4Cr	3.90	0.002	0.009	0.003	0.018	Balance
V-4Cr-1Ti	4.02	0.96	0.008	0.004	0.016	Balance
V-4Cr-2Ti	3.89	1.92	0.008	0.003	0.015	Balance
V-4Cr-3Ti	3.92	2.99	0.009	0.003	0.016	Balance
V-4Cr-4Ti	4.11	3.89	0.008	0.003	0.018	Balance

Note: Cr, Ti: inductively coupled plasma optical emission, C: combustion infrared absorption, N: Helium carrier fusion thermal conductivity, O: Helium carrier fusion infrared absorption.

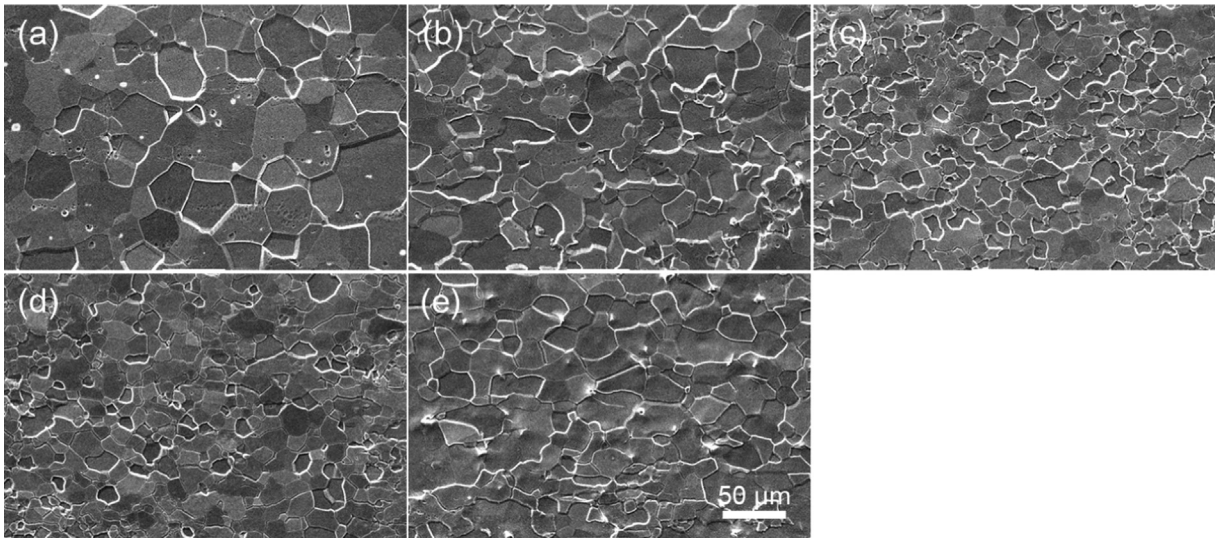

Fig. 1. SEM images of high-purity vanadium alloys with various Ti concentration: (a) V-4Cr, (b) V-4Cr-1Ti, (c) V-4Cr-2Ti, (d) V-4Cr-3Ti, and (e) V-4Cr-4Ti.

imens which were annealed at 1000 ℃ for 1 h, indicating completion of recrystallization. The grain size was estimated by several SEM images, and the average diameter as a function of Ti concentration is plotted in Fig. 2. The grain size decreases to the smallest, 12.2 ± 3.2 μm, with increasing Ti concentration up to 3 wt%. Then, it slightly increases to 14.6 ± 3.8 μm for the V-4Cr-4Ti alloy. In addition, the grain sizes of vanadium alloys with 2 – 4 wt% Ti addition are smaller in comparison with the V-4Cr and V-4Cr-1Ti alloys, indicating 2 wt% Ti and above would retard the migration of grain boundaries.

3.1.2. Precipitation

Fig. 3 shows bright-field TEM images of high-purity vanadium alloys with various Ti concentration. It is evidently noted that there are no precipitates in V-4Cr alloy, in contrast, precipitation occurs with higher Ti concentrations in V-4Cr-(1∼4)Ti alloys, suggesting that there is a threshold of Ti concentration for occurrence of precipitation in these high-purity vanadium alloys.

Fig. 4 shows the precipitate size distribution in V-4Cr-1Ti, V-4Cr-2Ti, V-4Cr-3Ti, and V-4Cr-4Ti alloys. Fig. 5 plots the corresponding average diameter and number density of precipitates as a function of Ti concentration. As can be seen, precipitates gradually coarsen from 38.1 ± 13.1 nm to 74.5 ± 25.9 nm as Ti concentration increases. By contrast, the number density of precipitates in V-4Cr-1Ti, V-4Cr-2Ti, and V-4Cr-3Ti alloys do not significantly change and keep at the same order of magnitude, 10^{19} m^{-3}. As for V-4Cr-4Ti alloy, it drops to 9.4 × 10^{18} m^{-3}, which is slightly lower than other V-4Cr-4Ti alloy containing higher interstitial impurities [28].

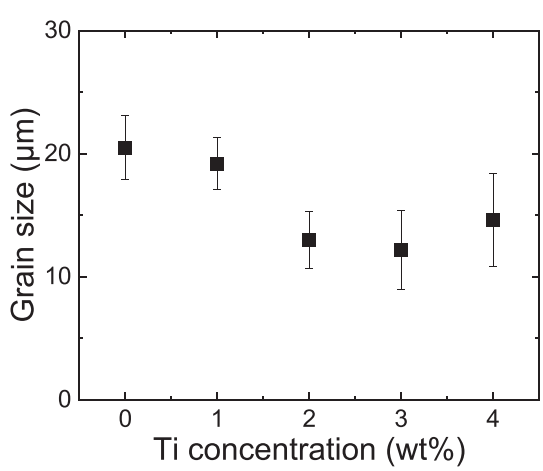

Fig. 2. Grain sizes of high-purity vanadium alloys dependence on the Ti concentration.

Fig. 6 shows the TEM images of precipitate and corresponding electron diffraction patterns in V-4Cr-1Ti alloy. According to the analysis on diffraction patterns, the precipitate is a fcc crystal structure with a lattice parameter of ∼0.433 nm. The orientation relationship between precipitates and matrix is $(111)_p//(110)_m$, and $[011]_p//[001]_m$, where subscript p and m denote precipitate and matrix, respectively. Ti(CON) particles with NaCl crystal structure are the common precipitates in V-4Cr-4Ti alloys, which are significantly affected by interstitial impurities and heat treatment conditions [29,30].

3.2. Vickers hardness and tensile properties

Fig. 7 shows the Vickers hardness of high-purity vanadium alloys with various Ti concentration. Vickers hardness of V-4Cr, V-4Cr-1Ti, V-4Cr-2Ti, V-4Cr-3Ti, and V-4Cr-4Ti alloys are 95 ± 2.4, 104.7 ± 2.2, 111.4 ± 4.4, 122.2 ± 3.3, and 137.3 ± 3.2, respectively. Note that the hardness gradually increases with increasing Ti concentration.

Fig. 8 summaries the tensile properties of high purity vanadium alloys tested at room temperature, such as ultimate tensile stress (UTS), yield stress (YS), total elongation (TE) and uniform elongation (UE). UTS and YS indicate a similar tendency on Ti concentration with Vickers hardness. The tensile strength gradually increases as increasing Ti concentration. V-4Cr-4Ti alloy has the highest UTS and YS, which are 389 ± 2 MPa, and 297 ± 6 MPa. With respect to elongation, TE of V-4Cr-2Ti alloy is 33.2 ± 4.6 % that is greater than others, and UE of the alloys is similar in the range of 15.6 – 17.4 %. In fact, both TE and UE do not evidently alter with increasing Ti concentration, indicating that there is no significant dependence upon Ti concentration for elongation at this range.

4. Discussions

It is generally known that there are several strengthening mechanisms in metals, such as solid solution strengthening (σ_{SS}),

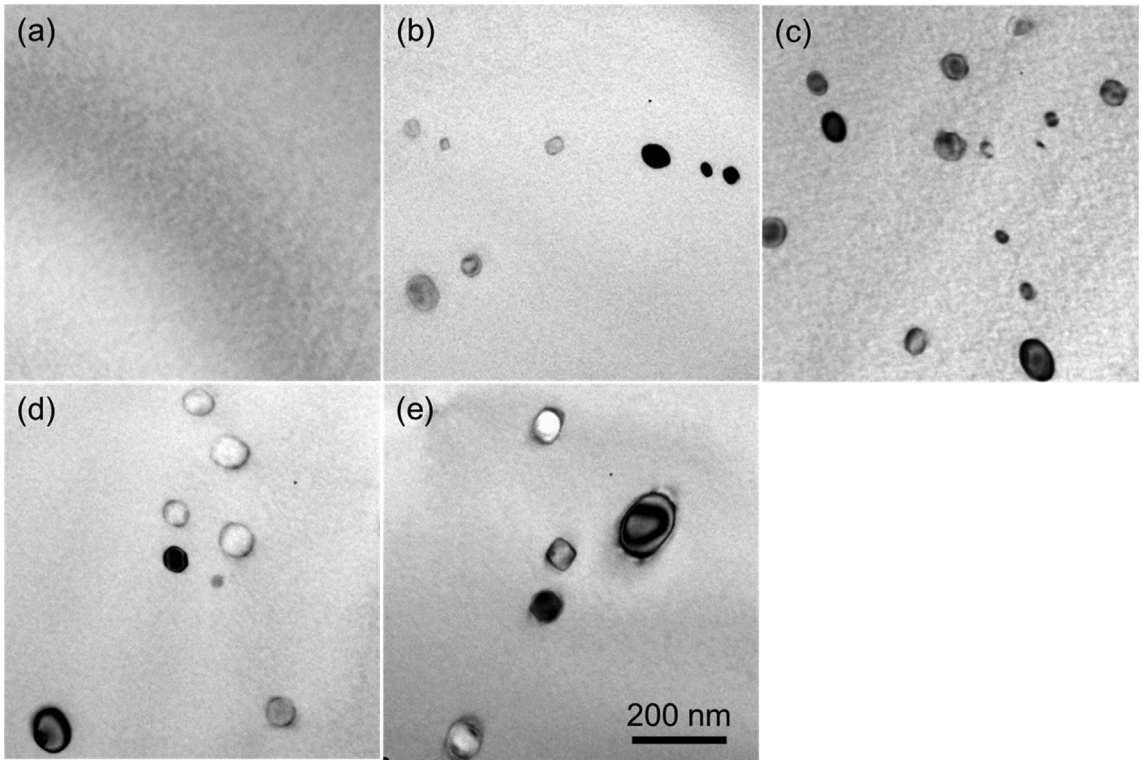

Fig. 3. Bright-field TEM images of high-purity vanadium alloys with various Ti concentration: (a) V-4Cr, (b) V-4Cr-1Ti, (c) V-4Cr-2Ti, (d) V-4Cr-3Ti, and (e) V-4Cr-4Ti.

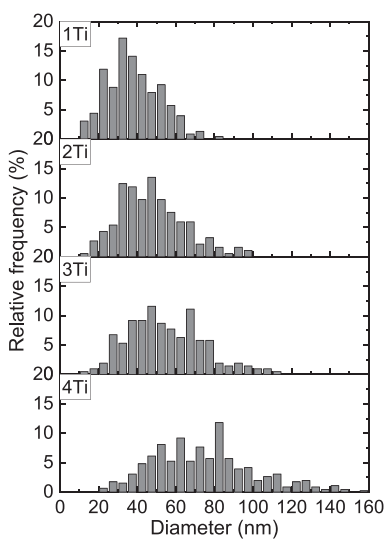

Fig. 4. Size distribution of precipitates in high-purity vanadium alloys with virous Ti concentration. Specimens from top to bottom are V-4Cr-1Ti, V-4Cr-2Ti, V-4Cr-3Ti, and V-4Cr-4Ti, respectively.

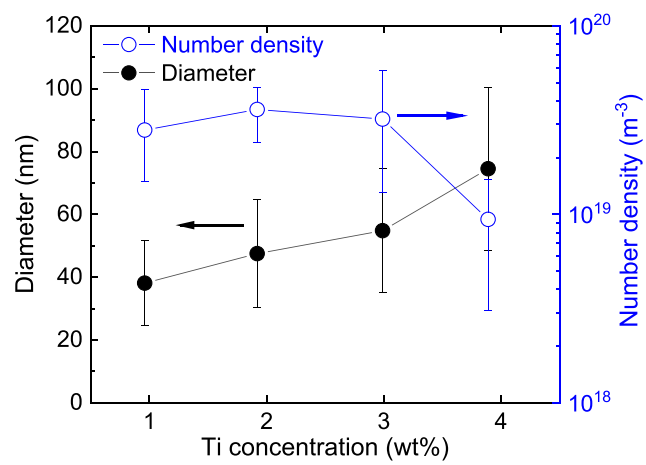

Fig. 5. Diameter and number density of precipitates in high-purity vanadium alloys as a function of Ti concentrations. Error bars for average diameter and number density indicate the standard deviation, and maximum and minimum, respectively.

grain boundary strengthening (σ_{GB}), precipitation strengthening (σ_P), and dislocation strengthening. Since all the vanadium alloys in this study were recrystallized, the dislocation density was so low that cannot be seen in TEM images, which is hereby neglectable for strengthening. Hence, the yield stress can be expressed by a linear summation of all the strengthening contributions as follows [31–35]:

$$\sigma_Y = \sigma_0 + \sigma_{SS} + \sigma_{GB} + \sigma_P \quad (1)$$

where σ_0 is friction stress of single crystal pure vanadium.

With respect to solid solution strengthening, interstitial impurities (i.e., C, N and O), Cr and Ti atoms serve as solute in the vanadium alloys. Due to occurrence of precipitation in V-4Cr-(1∼4)Ti alloys, it is therefore assumed that the interstitial impurities were scavenged out from the matrix and the precipitation strengthening would be considered instead of strengthening contributed by interstitial impurities.

Nagasaka et al. [36] investigated the effects of the nitrogen and oxygen concentrations on hardness of vanadium and the following equation for hardness estimation was deduced in the recrystallized vanadium.

$$H = H_0 + 0.12C_N + 0.057C_O \quad (2)$$

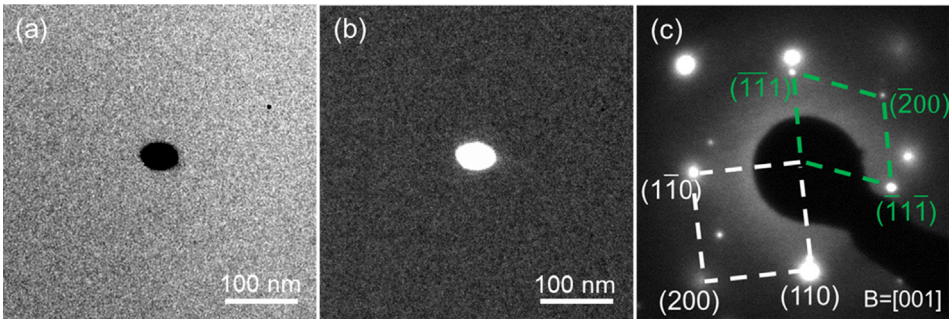

Fig. 6. Micrographs of a precipitate in V-4Cr-1Ti alloy. (a) Bright-field TEM image, (b) Dark-field TEM image, (c) Selected area diffraction pattern with indices of precipitate in green and matrix in white. (For interpretation of the references to colour in this figure legend, the reader is referred to the web version of this article.)

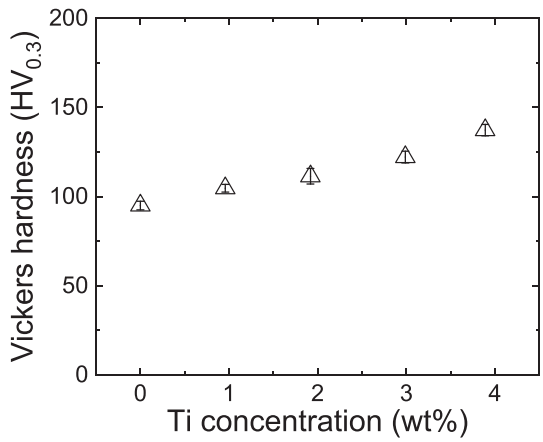

Fig. 7. Vickers hardness of high-purity vanadium alloys dependence on Ti concentration.

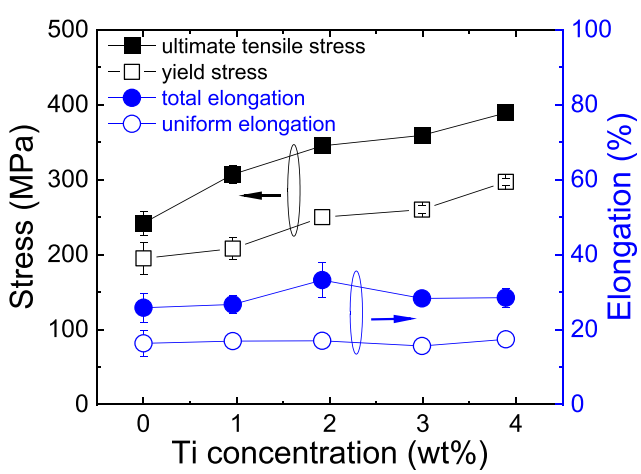

Fig. 8. Tensile properties of high-purity vanadium alloys at room temperature as a function of Ti concentration. Some error bars are so small that they are covered by the symbols.

where H_0 is a constant obtained by linear fitting, 48 kg·mm^{-2}, which is the hardness of vanadium containing carbon interstitials, C_N and C_O are nitrogen and oxygen concentration in wppm. Regarding strengthening from interstitials, Thompson et al. [7] reported that the hardness of vanadium markedly increased as rising N concentration, and carbon had a relatively little effect on hardness. Kainuma et al. [8] demonstrated that the strengthening potency at an equivalent concentration was different and the order was N > O > C. Besides, Harrod et al. [9] reported that carbon was about half as potent as nitrogen or oxygen for solid solution strengthening in vanadium. Obviously, the hardening coefficient of nitrogen is 2.1 times as high as that of oxygen in Equation (2). Therefore, it is reasonably assumed that the hardening coefficient of carbon is half of oxygen. The strengthening contribution from carbon is approximately 0.028 C_C, where C_C is carbon concentration. It is able to calculate the strengthening contribution from carbon, nitrogen and oxygen by substituting the concentration from Table 1.

It is noted that the calculated value via Equation (2) is Vickers hardness, which is needed to convert to strength in Equation (1). The unit of Vickers hardness is kg·mm^{-2}, which can be converted into MPa by multiplying 9.806 N·kg^{-1}. Fig. 9 plots Vickers hardness and yield stress of high-purity vanadium alloys. Equation (3) is established by linear fitting with R-square value of 0.998.

$$H_V = (4.605 \pm 0.09)\sigma_Y \tag{3}$$

where, both H_V and σ_Y are in MPa.

Based on Equations (2) and (3), the corresponding strengthening contributions from carbon, nitrogen, and oxygen in V-4Cr are 5.4 MPa, 7.7 MPa, and 21.8 MPa, respectively. Total strengthening contribution from interstitials (σ_{CNO}) is 34.9 MPa. Furthermore, the strength of single crystal pure vanadium can be estimated by subtracting the carbon strengthening from H_0, namely, σ_0 = 9.806 (H_0 − 0.028 C_C)/4.605 = 96.8 MPa. This value is smaller than that of vanadium in Refs. [7,8], because it is inevitable to eliminate all the foreign elements from the matrix, and some are polycrystalline including grain boundary strengthening. Additionally, the strength contributed from Cr atoms (σ_{Cr}) can be decided from the V-4Cr alloy with $\sigma_{Cr} = \sigma_Y - \sigma_0 - \sigma_{CNO} - \sigma_{GB}$, which is considered as the same in other alloys. Consequently, the strength contributed from

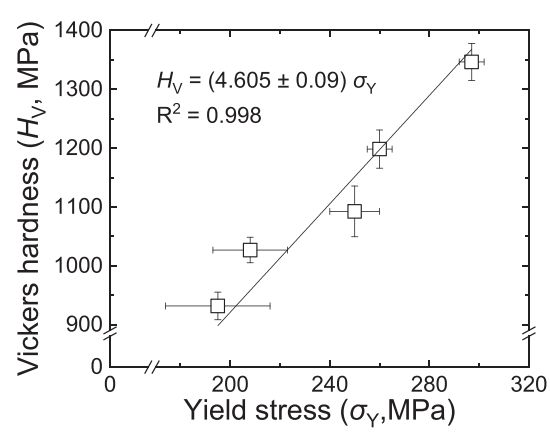

Fig. 9. Relationship between Vickers hardness (H_V) and yield stress (σ_Y) of high-purity vanadium alloys.

Table 2
Yield stress from tensile tests and strengthening contributions from calculation (MPa).

Specimens	Yield stress	σ_0	σ_{GB}	σ_{CNO}	σ_{Cr}	σ_P	σ_{Ti}
V-4Cr	195	96.8	46.2 ± 1.5	34.9	17.1 ± 1.5	–	–
V-4Cr-1Ti	208	96.8	47.7 ± 2.7	–	17.1 ± 1.5	11.5 ± 2.4	34.9 ± 6.6
V-4Cr-2Ti	250	96.8	58.0 ± 11.4	–	17.1 ± 1.5	14.6 ± 2.6	63.5 ± 15.5
V-4Cr-3Ti	260	96.8	59.8 ± 6.4	–	17.1 ± 1.5	14.7 ± 2.5	71.5 ± 10.4
V-4Cr-4Ti	297	96.8	54.7 ± 2.6	–	17.1 ± 1.5	11.9 ± 1.5	116.5 ± 5.6

Ti atoms in other alloys can be calculated by $\sigma_{Ti} = \sigma_Y - \sigma_0 - \sigma_{Cr} - \sigma_{GB} - \sigma_P$.

With respect to the grain boundary strengthening, Hall-Petch relationship [37,38] is widely utilized to determine the strength increment in polycrystalline materials.

$$\sigma_{GB} = k_{H-P} D^{-1/2} \tag{4}$$

where k_{H-P} is Hall-Petch coefficient, whose value is 209 MPa·μm$^{1/2}$ [39] for recrystallized vanadium, and D is the average grain size, which is shown in Fig. 2.

Regarding precipitation strengthening, the precipitates can act as barriers to impede the movements of dislocations. Orowan's model [40] is generally used to describe the strengthening contribution as follows:

$$\sigma_P = \alpha M \mu b (Nd)^{1/2} \tag{5}$$

where α is the obstacle strength of the precipitates, M is Taylor factor (3.06 [40] for polycrystalline bcc metals), μ is the shear modulus of the matrix (46.7 GPa [41]), b is the magnitude of Burgers vector (0.26 nm [41]), N is the number density of precipitates, and d is the average diameter of precipitates shown in Fig. 5. The obstacle strength α is estimated by the critical bowing angle when a dislocation propagates through the obstacle. In principle, the value of α is equal to 1 for the impenetrable particles, whereas it is generally used as 0.81 – 0.84 for a random distribution [42]. By contrast, for the penetrable particles, α is smaller than 0.8, such as irradiation-induced dislocation loops, defect clusters [12]. As shown in Fig. 6, there exists evident orientation relationship between precipitates and the matrix, indicating the coherent and penetrable precipitates. Tougou et al. [43] analyzed the obstacle strength of Ti(CON) precipitates in V-4Cr-4Ti alloy via *in situ* TEM observations and determined the average obstacle strength as α = 0.3, which is taken in this study.

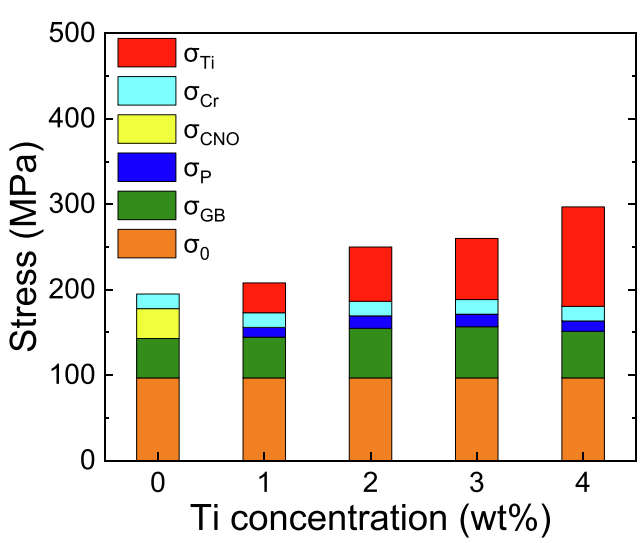

Fig. 10. Strength contributions from friction stress of single crystal vanadium (σ_0), solid solution strengthening (σ_{CNO}, σ_{Cr}, σ_{Ti}), grain boundary strengthening (σ_{GB}), and precipitation strengthening (σ_P) in high-purity vanadium alloys with various Ti concentration. The total stress values correspond to the yield stress of the high-purity V-4Cr-xTi alloys.

Table 2 lists the calculated values from grain boundary strengthening (σ_{GB}), precipitation strengthening (σ_P) and solid solution strengthening (σ_{CNO}, σ_{Cr}, and σ_{Ti}).

Fig. 10 separately plots the corresponding strength contributors in columns as a function of Ti concentration. It is clearly seen that the sequence of strengthening contribution in V-4Cr-(1∼4)Ti alloys is $\sigma_{SS} > \sigma_{GB} > \sigma_P$. With respect to solid solution strengthening from Ti, it gradually increases with increasing Ti concentration, leading to the highest value in V-4Cr-4Ti alloy. Precipitation strengthening is the lowest strength contributor and not obviously changed upon Ti concentration, suggesting that 1 wt% Ti addition in the high purity vanadium is proper for scavenging the interstitial impurities, and results in comparable precipitation strengthening with V-4Cr-4Ti alloy.

5. Conclusions

The effects of Ti concentration on microstructure and mechanical properties of high-purity V-4Cr-xTi alloys are systematically investigated by SEM, TEM, Vickers hardness and tensile tests. The following conclusions can be drawn:

(1) Precipitates are observed in high-purity vanadium alloys with 1 wt% Ti and above, whose size increases with increasing Ti concentration.
(2) Both Vickers hardness and tensile strength gradually increases with increasing Ti concentration.
(3) Strengthening mechanisms for the recrystallized vanadium alloys are comprised of solid solution strengthening (σ_{SS}), grain boundary strengthening (σ_{GB}), and precipitation strengthening (σ_P). The sequence of strength contributors is $\sigma_{SS} > \sigma_{GB} > \sigma_P$. Solid solution strengthening from Ti increases with increasing Ti concentration, and precipitation strengthening is not obviously dependent upon Ti concentration.
(4) Ti concentration is reasonably reduced to 1 wt% for scavenging the interstitial impurities and providing comparable precipitation strengthening with V-4Cr-4Ti alloy.

Data availability

Data will be made available on request.

Declaration of Competing Interest

The authors declare that they have no known competing financial interests or personal relationships that could have appeared to influence the work reported in this paper.

Acknowledgements

This work was supported by the Fusion Engineering Research Project of National Institute for Fusion Science, Japan (Budget code:

UFFF023), JSPS KAKENHI Grant Numbers JP20H00144 and JP20K14445, and the inter-university cooperative research program of the Cooperative Research and Development Center for Advanced Materials, Institute for Materials Research, Tohoku University (Proposal No.: 202112-CRKEQ-0029). The author J.J. Shen is grateful to Mr. D. Nagata's assistance for TEM observations.

References

[1] B.A. Loomis, D.L. Smith, Vanadium alloys for structural applications in fusion systems: a review of vanadium alloy mechanical and physical properties, J. Nucl. Mater. 191 (Part A) (1992) 84–91.
[2] D.L. Smith, M.C. Billone, K. Natesan, Vanadium-base alloys for fusion first-wall/blanket applications, Int. J. Refract. Met. Hard Mater. 18 (4) (2000) 213–224.
[3] T. Muroga, T. Nagasaka, K. Abe, V.M. Chernov, H. Matsui, D.L. Smith, Z.Y. Xu, S.J. Zinkle, Vanadium alloys – overview and recent results, J. Nucl. Mater. 307 (Part 1) (2002) 547–554.
[4] T. Muroga, J.M. Chen, V.M. Chernov, R.J. Kurtz, M. Le Flem, Present status of vanadium alloys for fusion applications, J. Nucl. Mater. 455 (1) (2014) 263–268.
[5] D.L. Smith, H.M. Chung, B.A. Loomis, H.C. Tsai, Reference vanadium alloy V-4Cr-4Ti for fusion application, J. Nucl. Mater. 233–237 (1996) 356–363.
[6] H.M. Chung, B.A. Loomis, D.L. Smith, Development and testing of vanadium alloys for fusion applications, J. Nucl. Mater. 239 (Supplement C) (1996) 139–156.
[7] R.W. Thompson, O.N. Carlson, Effect of nitrogen and carbon on the low-temperature embrittlement of vanadium, Journal of the Less Common Metals 9 (5) (1965) 354–361.
[8] T. Kainuma, N. Iwao, T. Suzuki, R. Watanabe, Effects of oxygen, nitrogen and carbon additions on the mechanical properties of vanadium and V/Mo alloys, J. Nucl. Mater. 80 (2) (1979) 339–347.
[9] D.L. Harrod, R.E. Gold, Mechanical properties of vanadium and vanadium-base alloys, International Metals Reviews 25 (1) (1980) 163–211.
[10] M.-G. Jo, P.P. Madakashira, J.-Y. Suh, H.N. Han, Effect of oxygen and nitrogen on microstructure and mechanical properties of vanadium, Materials Science and Engineering: A 675 (2016) 92–98.
[11] M. Satou, K. Abe, H. Kayano, H. Takahashi, Low swelling behavior of V-Ti-Cr-Si-type alloys, J. Nucl. Mater. 191–194 (1992) 956–959.
[12] P.M. Rice, S.J. Zinkle, Temperature dependence of the radiation damage microstructure in V–4Cr–4Ti neutron irradiated to low dose, J. Nucl. Mater. 258–263 (1998) 1414–1419.
[13] H. Watanabe, T. Arinaga, K. Ochiai, T. Muroga, N. Yoshida, Microstructure of vanadium alloys during ion irradiation with stepwise change of temperature, J. Nucl. Mater. 283–287 (2000) 286–290.
[14] K.-I. Fukumoto, H. Matsui, Y. Candra, K. Takahashi, H. Sasanuma, S. Nagata, K. Takahiro, Radiation-induced precipitation in V–(Cr, Fe)–Ti alloys irradiated at low temperature with low dose during neutron or ion irradiation, J. Nucl. Mater. 283–287 (2000) 535–539.
[15] H. Watanabe, M. Suda, T. Muroga, N. Yoshida, Oxide formation of a purified V–4Cr–4Ti alloy during heat treatment and ion irradiation, J. Nucl. Mater. 307–311 (2002) 408–411.
[16] K.-I. Fukumoto, H. Matsui, H. Ohkubo, Z. Tang, Y. Nagai, M. Hasegawa, Identification of ultra-fine Ti-rich precipitates in V-Cr–Ti alloys irradiated below 300°C by using positron CDB technique, J. Nucl. Mater. 373 (1–3) (2008) 289–294.
[17] T. Muroga, T. Nagasaka, Reduction of impurity levels of vanadium and its alloys for fusion application, Int. J. Refract. Met. Hard Mater. 18 (4) (2000) 225–230.
[18] T. Muroga, T. Nagasaka, A. Iiyoshi, A. Kawabata, S. Sakurai, M. Sakata, NIFS program for large ingot production of a V-Cr–Ti alloy, J. Nucl. Mater. 283–287 (2000) 711–715.
[19] T. Nagasaka, T. Muroga, Y. Wu, Z. Xu, M. Imamura, Low Activation Characteristics of Several Heats of V-4Cr-4Ti Ingot, Journal of Plasma and Fusion Research SERIES 5 (2002) 545–550.
[20] T. Muroga, Vanadium Alloys for Fusion Blanket Applications, MATERIALS TRANSACTIONS 46 (3) (2005) 405–411.
[21] N. Takuya, M. Takeo, F. Ken-ichi, W. Hideo, L.G. Martin, C. Jiming, Development of fabrication technology for low activation vanadium alloys as fusion blanket structural materials, Nucl. Fusion 46 (5) (2006) 618.
[22] D.R. Diercks, B.A. Loomis, Alloying and impurity effects in vanadium-base alloys, J. Nucl. Mater. 141–143 (1986) 1117–1124.
[23] B.A. Loomis, D.L. Smith, F.A. Garner, Swelling of neutron-irradiated vanadium alloys, J. Nucl. Mater. 179 (Part 1) (1991) 771–774.
[24] H. Matsui, K. Fukumoto, D.L. Smith, H.M. Chung, W. van Witzenburg, S.N. Votinov, Status of vanadium alloys for fusion reactors, J. Nucl. Mater. 233 (Part 1) (1996) 92–99.
[25] K. Fukumoto, A. Kimura, H. Matsui, Swelling behavior of V-Fe binary and V–Fe–Ti ternary alloys, J. Nucl. Mater. 258–263 (1998) 1431–1436.
[26] G.J. Butterworth, K.A. McCarthy, G.R. Smolik, C.B.A. Forty, Safety and environmental aspects of vanadium alloys, J. Nucl. Mater. 212–215 (1994) 667–672.
[27] E.T. Cheng, Waste management aspect of low activation materials, Fusion Eng. Des. 48 (3) (2000) 455–465.
[28] K. Sakai, M. Satou, M. Fujiwara, K. Takanashi, A. Hasegawa, K. Abe, Mechanical properties and microstructures of high-chromium V-Cr–Ti type alloys, J. Nucl. Mater. 329 (Part A) (2004) 457–461.
[29] T. Nagasaka, N.J. Heo, T. Muroga, M. Imamura, Examination of fabrication process parameters for improvement of low-activation vanadium alloys, Fusion Eng. Des. 61–62 (2002) 757–762.
[30] N.J. Heo, T. Nagasaka, T. Muroga, Recrystallization and precipitation behavior of low-activation V-Cr–Ti alloys after cold rolling, J. Nucl. Mater. 325 (1) (2004) 53–60.
[31] E. Hornbogen, E.A. Starke, Theory assisted design of high strength low alloy aluminum, Acta Metallurgica et Materialia 41 (1) (1993) 1–16.
[32] Q. Li, Modeling the microstructure-mechanical property relationship for a 12Cr-2W-V-Mo-Ni power plant steel, Materials Science and Engineering: A 361 (1–2) (2003) 385–391.
[33] N. Kamikawa, K. Sato, G. Miyamoto, M. Murayama, N. Sekido, K. Tsuzaki, T. Furuhara, Stress–strain behavior of ferrite and bainite with nano-precipitation in low carbon steels, Acta Mater. 83 (2015) 383–396.
[34] J.J. Shen, Y.F. Li, F. Li, H.L. Yang, Z.S. Zhao, S. Kano, Y. Matsukawa, Y. Satoh, H. Abe, Microstructural characterization and strengthening mechanisms of a 12Cr-ODS steel, Mat Sci Eng a-Struct 673 (2016) 624–632.
[35] Y. Matsukawa, H.L. Yang, K. Saito, Y. Murakami, T. Maruyama, T. Iwai, K. Murakami, Y. Shinohara, T. Kido, T. Toyama, Z. Zhao, Y.F. Li, S. Kano, Y. Satoh, Y. Nagai, H. Abe, The effect of crystallographic mismatch on the obstacle strength of second phase precipitate particles in dispersion strengthening: bcc Nb particles and nanometric Nb clusters embedded in hcp Zr, Acta Mater. 102 (2016) 323–332.
[36] T. Nagasaka, H. Takahashi, T. Muroga, T. Tanabe, H. Matsui, Recovery and recrystallization behavior of vanadium at various controlled nitrogen and oxygen levels, J. Nucl. Mater. 283 (Part 2) (2000) 816–821.
[37] E.O. Hall, The deformation and ageing of mild steel, Proc. Phys. Soc. B 64 (1951) 747–753.
[38] N.J. Petch, The cleavage strength of polycrystals, J. Iron Steel Inst. 174 (1953) 25–28.
[39] Y.B. Chun, S.H. Ahn, D.H. Shin, S.K. Hwang, Combined effects of grain size and recrystallization on the tensile properties of cryorolled pure vanadium, Materials Science and Engineering: A 508 (1) (2009) 253–258.
[40] R.E. Stoller, S.J. Zinkle, On the relationship between uniaxial yield strength and resolved shear stress in polycrystalline materials, J. Nucl. Mater. 283–287 (2000) 349–352.
[41] T. Nagasaka, T. Muroga, H. Watanabe, K. Yamasaki, N.-J. Heo, K. Shinozaki, M. Narui, Recovery of Hardness, Impact Properties and Microstructure of Neutron-Irradiated Weld Joint of a Fusion Candidate Vanadium Alloy, MATERIALS TRANSACTIONS 46 (3) (2005) 498–502.
[42] A.J.E. Foreman, M.J. Makin, Dislocation movement through random arrays of obstacles, The Philosophical Magazine: A Journal of Theoretical Experimental and Applied Physics 14 (131) (1966) 911–924.
[43] K. Tougou, K. Nogiwa, K. Tachikawa, K.-I. Fukumoto, Tensile testing study of dynamic interactions between dislocations and precipitate in vanadium alloys, J. Nucl. Mater. 442 (1, Supplement 1) (2013) S350–S353.